



UNIVERSITY OF LEEDS

This is a repository copy of *Mutations in the polyglutamylase gene TTLL5, expressed in photoreceptor cells and spermatozoa, are associated with cone-rod degeneration and reduced male fertility.*

White Rose Research Online URL for this paper:
<http://eprints.whiterose.ac.uk/104506/>

Version: Accepted Version

Article:

Bedoni, N, Haer-Wigman, L, Vaclavik, V et al. (28 more authors) (2016) Mutations in the polyglutamylase gene TTLL5, expressed in photoreceptor cells and spermatozoa, are associated with cone-rod degeneration and reduced male fertility. *Human Molecular Genetics*, 25 (20). pp. 4546-4555. ISSN 0964-6906

<https://doi.org/10.1093/hmg/ddw282>

© The Author 2016. Published by Oxford University Press. This is an author produced version of a paper published in *Human Molecular Genetics*. Uploaded in accordance with the publisher's self-archiving policy.

Reuse

Items deposited in White Rose Research Online are protected by copyright, with all rights reserved unless indicated otherwise. They may be downloaded and/or printed for private study, or other acts as permitted by national copyright laws. The publisher or other rights holders may allow further reproduction and re-use of the full text version. This is indicated by the licence information on the White Rose Research Online record for the item.

Takedown

If you consider content in White Rose Research Online to be in breach of UK law, please notify us by emailing eprints@whiterose.ac.uk including the URL of the record and the reason for the withdrawal request.



eprints@whiterose.ac.uk
<https://eprints.whiterose.ac.uk/>

Mutations in the polyglutamylase gene *TLL5*, expressed in photoreceptor cells and spermatozoa, are associated with cone-rod degeneration and reduced male fertility

Nicola Bedoni,^{1§} Lonneke Haer-Wigman,^{2,3§} Veronika Vaclavik,^{4,5} Hoai Viet Tran,⁴ Pietro Farinelli,¹ Sara Balzano,¹ Beryl Royer-Bertrand,^{1,6} Mohammed E. El-Asrag,⁷ Olivier Bonny,⁸ Christos Ikonomidis,⁹ Yan Litzistorf,⁹ Konstantinos Nikopoulos,¹ Georgia Yiotti,¹⁰ Maria Stefanidou,¹⁰ Martin McKibbin,¹¹ Jamie Ellingford,¹³ Adam P. Booth,¹² Graeme Black,¹¹ Carmel Toomes,⁷ Chris F. Inglehearn,⁷ Carel B. Hoyng,¹⁴ Nathalie Bax,¹⁴ Caroline C.W. Klaver,^{14,15} Alberta A. Thiadens,¹⁵ Fabien Murisier,¹⁶ Daniel F. Schorderet,¹⁷ Manir Ali,⁷ Frans P.M. Cremers,^{2,3} Sten Andréasson,¹⁸ Francis L. Munier^{4§} and Carlo Rivolta^{1§*}

¹ Department of Computational Biology, Unit of Medical Genetics, University of Lausanne, Lausanne, Switzerland

² Department of Human Genetics, Radboud University Medical Center, Nijmegen, The Netherlands

³ Donders Institute for Brain, Cognition and Behaviour, Radboud University, Nijmegen, the Netherlands

⁴ Jules Gonin Eye Hospital, Lausanne, Switzerland

⁵ Department of Ophthalmology, Fribourg Hospital HFR, Fribourg, Switzerland

⁶ Center for Molecular Diseases, Department of Pediatrics, Lausanne University Hospital (CHUV), Lausanne, Switzerland

⁷ Section of Ophthalmology & Neuroscience, Leeds Institute of Biomedical & Clinical Sciences, University of Leeds, Leeds, United Kingdom

⁸ Service of Nephrology, Lausanne University Hospital (CHUV), Lausanne, Switzerland

⁹ Department of Otorhinolaryngology, Head and Neck Surgery, Lausanne University Hospital (CHUV), Lausanne, Switzerland

¹⁰ Department of Ophthalmology, University of Ioannina School of Medicine, Ioannina, Greece

¹¹ The Eye Department, St. James's University Hospital, Leeds, United Kingdom

¹² Royal Eye Infirmary, Derriford Hospital, Plymouth, United Kingdom

¹³ Manchester Centre for Genomic Medicine, University of Manchester, St Mary's Hospital, Manchester, United Kingdom

¹⁴ Department of Ophthalmology, Radboud University Medical Center, Nijmegen, The Netherlands

¹⁵ Department of Ophthalmology, Erasmus Medical Center, Rotterdam, The Netherlands

¹⁶ Fertas Andrology Laboratory, Lausanne, Switzerland

¹⁷ Institute for Research in Ophthalmology, University of Lausanne and Ecole Polytechnique Federale of Lausanne, Switzerland

¹⁸ Department of Ophthalmology, Lund University, Lund, Sweden

§equal contribution

*correspondence:

Carlo Rivolta, Ph.D.

Department of Computational Biology
Unit of Medical Genetics
University of Lausanne
Rue du Bugnon 27
1011 Lausanne
Switzerland

Phone: +41-21-6925451

Fax: +41-21-6925455

Email: carlo.rivolta@unil.ch

ABSTRACT

Hereditary retinal degenerations encompass a group of genetic diseases characterized by extreme clinical variability. Following next-generation sequencing and autozygome-based screening of patients presenting with a peculiar, recessive form of cone-dominated retinopathy, we identified five homozygous variants [p.(Asp594fs), p.(Gln117*), p.(Met712fs), p.(Ile756Phe), and p.(Glu543Lys)] in the polyglutamylase-encoding gene *TLL5*, in eight patients from six families. The two male patients carrying truncating *TLL5* variants also suffered from a substantial reduction in sperm motility and infertility, whereas those carrying missense changes were fertile. Defects in this polyglutamylase in humans have recently been associated with cone photoreceptor dystrophy, while mouse models carrying truncating mutations in the same gene also display reduced fertility in male animals. We examined the expression levels of *TLL5* in various human tissues and determined that this gene has multiple viable isoforms, being highly expressed in testis and retina. In addition, antibodies against *TLL5* stained the basal body of photoreceptor cells in rat and the centrosome of the spermatozoon flagellum in humans, suggesting a common mechanism of action in these two cell types. Taken together, our data indicate that mutations in *TLL5* delineate a novel, allele-specific syndrome causing defects in two as yet pathogenically unrelated functions, reproduction and vision.

INTRODUCTION

Cone dystrophies (CDs) and cone-rod dystrophies (CRDs) are rare heterogeneous retinal disorders with an estimated prevalence of ~1:40,000 (1). They lead to severe visual impairment, primarily or exclusively due to the degeneration of cone photoreceptors. Patients experience progressive loss of visual acuity, defective color vision, photophobia, and have central scotomas. Only later, as the disease progresses, in some cases loss of peripheral vision may also occur (2, 3).

The progressive degeneration of retinal photoreceptors in CDs and CRDs is mostly nonsyndromic and has been associated with multiple genetic causes, with at least 20 associated disease genes (RetNet; <http://www.sph.uth.tmc.edu/RetNet/>). However, more than 75% of cases presenting with dominant or recessive forms of these conditions are genetically unsolved (4). Recent discoveries in CD molecular genetics include the identification of pathogenic variants in the tubulin polyglutamylase *TLL5* (Tubulin Tyrosine Ligase-like Protein 5) gene, found to cause retinal dystrophy in four British families (5). This gene, like the 12 other members of the TLL superfamily, is involved in post-translational modifications of α - and β -tubulin, which are components of the axonemes of both cilia and flagella.

Interestingly, male mice with a defective *TLL5* display dramatically reduced fertility associated with defects in sperm motility (6). Most sperm tails of mutant mice were found to have disrupted axonemes with loss of tubulin doublets and a significantly decreased polyglutamylation in the upper and lower segments. No abnormal phenotype of retinal photoreceptors or of cochlear cells was initially observed, based on histologic examination (6). A second study with a more

thorough characterization of the ocular phenotype in the same mouse model showed a decline of electroretinographic (ERG) amplitudes for both rods and cones in aged mice (20-22 mo). However, no microtubule defects were found after examination of electron micrographs (7).

Ciliopathies represent a class of hereditary disorders involving deficiencies in ciliary and cilia-associated proteins, often affecting a variety of tissues and organs (8). Due to the presence of an immotile cilium in both rods and cones photoreceptors, many ciliopathies display a retinal phenotype, either as part of a syndromic condition (associated with hearing defects, renal nephronophtisis, liver fibrosis, bone and/or brain anomalies) or as the sole pathological sign (9-11).

Following the investigation of a cohort of patients displaying CD or CRD, we identified mutations in *TLL5* that are associated with both retinal degeneration and reduced sperm motility in humans, possibly defining a novel syndromic ciliopathy.

RESULTS

Clinical and molecular findings

Our research started with the molecular characterization of a Swiss male patient (P1), aged 75 years, presenting with a late-onset cone dystrophy (CD). He was the eldest of three brothers and his parents were first cousins (Figure 1, F1), without any history of ocular problems. The patient was first seen at the age of 33 years, when he first noticed blurred vision. His best corrected Snellen visual acuity (BCVA) at that time was 0.6 in the right eye and 0.8 in his left eye. Seven years later, his BCVA was still stable, but worsened when he was 53 years old, dropping dramatically to 0.05 in the right eye and 0.08 in the left eye. He was also complaining of a reduced dark adaptation. Twenty-two years later his vision remained stable, with the patient using more of his peripheral vision.

The clinical examination was typical of a cone dystrophy: the fundus examination showed central foveal atrophy with peripapillary hyperpigmentation and atrophy, while the peripheral retina was within normal limits (Figure 2). The first ERGs (performed when the patient was 56 years old) showed normal scotopic responses, whereas photopic responses had severely reduced amplitude. The following ERG testing, when the patient was 70 years old, showed some rod involvement, with reduced rod-specific b-wave. The 30-Hz flicker was undetectable. Autofluorescent (AF) images at age 66 years (Figure 2) showed central hypofluorescence corresponding to atrophy, surrounded by a large hyperfluorescent ring. AF imaging at age 72 indicated that the ring mildly increased in diameter, and so did the area of hypofluorescence (Figure 2). Kinetic

visual field tested at this later age showed mild constriction and central scotoma in both eyes.

The DNA of the patient was first screened for mutations in known disease genes. Following the negative output of a panel-based Next-Generation Sequencing screening [the IROme (12)], we performed whole-genome sequencing (WGS) of the patient's DNA. This latter procedure resulted in more than 4 million DNA variants with respect to the human reference genome (Build hg19). These were evaluated by the use of an internal *in-silico* pipeline assessing their frequency in the general population, quality, etc. (Table S1), as well as their presence within autozygous regions (Figure S1). At the end of this process, we were left with 19 variants (7 in autozygous regions), including c.1782delT in *TTL5* (Figure 3), a gene known to be involved in microtubule posttranslational modifications and associated with ciliary microtubule stabilization (13). The variant was in exon 20 and consisted of a 1-bp deletion causing a frameshift starting from codon 594 and terminating with the creation of a premature stop triplet 29 codons downstream [p.(Asp594Glufs*29)]. It was also not detected in the genome of 400 healthy controls from the same geographic region of Switzerland [data from the CoLaus study (14)], and from publicly available databases [ExAC (15), dbSNP (16)]. Importantly, this DNA change localized to a region of chromosome 14 (75,986,579-80,875,911, Build hg19) showing clear autozygosity (Figure S1) in P1's genome. Because of the possible involvement of *TTL5* in extra-ocular ciliary functions, the patient underwent more detailed clinical examinations. To assess the presence of additional subtle abnormalities in organs known to be affected by ciliopathies, he was evaluated for both renal and otorhinolaryngological functions. He did not display the classical clinical features

of renal ciliopathy (no polyuria/polydipsia), but chronic renal insufficiency without proteinuria (stage G3aA1) (17) was identified, associated with low-grade chronic anemia. By ultrasound, the size of the kidneys appeared to be preserved, but a small asymmetry was noted (9.6 cm on the left vs. 10.7 cm on the right side), without significant renal artery stenosis. No cysts were visible and no biopsy was performed. Altogether, the renal features were consistent with age-related decreased renal function, but low-grade and late appearance nephronophthisis cannot be fully excluded. The observed minor sensorineural hearing loss, and loss of some high frequencies, was compatible with the natural course of hearing on a person of the age of the subject (Figure S2). The clinical examination and patient's history did not reveal any upper airway pathology necessitating further investigations for impaired mucociliary function in the sinus or the bronchi. The patient reported history of infertility due to reduced sperm motility, diagnosed when he was in his late 20's. He could not have offspring and adopted two children. Following our findings, a new semen analysis was performed at age 75, revealing azoospermia, a sign that nonetheless could simply be related to the difficulty in obtaining an ejaculate at his current age.

Based on these findings, we extended our analyses to a number of additional cohorts of 365 patients with CD and CRD from Switzerland, Sweden, Greece, The Netherlands, and Britain. In a Swedish male patient of Iraqi descent (P2), we identified the homozygous nonsense variant c.349C>T;p.(Gln117*) by targeted Sanger sequencing of *TTL5* (Figure 1, F2; Figure 3). Again, this variant was absent from controls and publicly available databases. Although the patient did not report any history of consanguinity, the occurrence of this extremely rare variant in a homozygous state suggests the presence of residual consanguinity or of a

geographical founder effect, which was not tested at the genome level. The patient, aged 46 years, reported no family history of similar visual impairment. Fundus examination revealed degenerative changes, especially in the posterior pole, but more normal features in the periphery. Visual field analysis by Goldmann perimetry showed residual fields in the periphery, but a large central scotoma. Full-field ERG demonstrated residual cone and rod response, consistent with a diagnosis of cone-rod degeneration. In addition to these signs and symptoms typical of CRD, the patient had high myopia (Table 1). This subject was also infertile, but had been able to have a child by *in vitro* fertilization. His semen analysis revealed a normal spermatozoa count but, similar to P1, reduced sperm motility. He also had morphologically normal spermatozoa for 5% of the count, over three independent assays.

Following autozygome-based analysis (Figure S1), we identified homozygous mutations in three additional patients from the Netherlands (Figure 1, F3-5). All of them were diagnosed with CD, with full-field ERGs showing reduction of cone function but preserved rod responses (Table 1). Similar to the cases described above, the female patient P3 had a *TLL5* truncating mutation, c.2132_2133insGATA;p.(Met712IleAspfs*15), resulting in a premature termination codon. The other two patients (P4, and P5) were males and both carried homozygous missense mutations, namely c.1627G>A;p.(Glu543Lys) and c.2266A>T;p.(Ile756Phe), respectively (Figure 3). Following color vision testing, substantial mistakes were made in all three color axes. All patients had a myopic refractive error, but none of them showed any additional extraocular symptoms. In particular, they did not report any fertility problems, and both male patients had offspring.

Finally, a male patient (P6) of Pakistani origin was screened by whole-exome sequencing (WES). He was a member of a consanguineous pedigree that included six additional individuals with high myopia and an acquired CD or CRD with loss of corrected visual acuity from the second decade onwards (Figure 1, F6). In this case as well, a homozygous mutation in *TLL5* was identified within an autozygous region in chromosome 14 (Figure S1). It was the same missense detected above [c.1627G>A;p.(Glu543Lys), Figure 3], which perfectly cosegregated with the disease in the three affected and two unaffected individuals for which DNA samples were available. Of note, in addition to retinal dystrophy, all patients from this pedigree reported high to very-high myopia (-5 to -22 diopters) (Table 1). None of the patients reported fertility problems, and indeed patient P6 had five children.

***TLL5* RNA isoforms and expression in different tissues.**

According to publicly-available databases, *TLL5* produces six protein-coding and alternatively spliced isoforms (transcripts 001, 002, 003, 016, 017, 018 of the Ensembl database GRCh37, release 84), presenting a rather widespread expression throughout different tissues and organs (UniGene). To gain insights into this topic, we investigated the composition and abundance of *TLL5* transcripts from a panel of cadaveric organs and tissues (Figure 4).

Our data confirmed that *TLL5* has an extremely variable expression pattern, both in terms of isoforms and of presence in various tissues. However, qualitative and quantitative assessment of all transcripts revealed that expression of the canonical isoform 001 was overwhelmingly more abundant (more than 40-fold higher than the average of the remainder) and that expression in retina and testis

represented ~64% of *TLL5* presence across all tissues and organs examined (31 and 33% in testis and retina, respectively; Figure 4). Interestingly, all mutations identified in our cohort of patients affected isoform 001, and individuals with inactivating mutations show reduced fertility (Table 1).

***TLL5* mRNA level in the index patient**

Since mutations leading to premature termination codons trigger nonsense-mediated mRNA decay (NMD) and result in no or in short-lived transcripts (18), we analyzed expression of *TLL5* in skin fibroblasts from patient P1, displaying retinal degeneration and infertility. Quantitative real time PCR (q-PCR) resulted in a dramatically reduced detection of the transcript of interest as compared to a healthy control fibroblast mRNA (~10%; Figure 5).

***TLL5* protein in ciliated fibroblasts, retina, and spermatozoa**

To better understand the role of *TLL5* with respect to the cellular cilium, we analyzed control fibroblasts following serum starvation, a procedure that induces ciliogenesis. Immunofluorescence analysis revealed clear localization of *TLL5* at both centrioles (Figure 6, panels A-D).

Subsequently, we performed immunofluorescence analyses in retina and sperm cells from rat and human, respectively (Figure 6, panels E-G). In agreement with previous results in mouse and human (5), the anti-*TLL5* antibody decorated the inner segment of photoreceptors in proximity of the basal body and the connecting cilium, suggesting that *TLL5* may in fact play its functions at the base of the photoreceptor primary cilium.

Staining of mature human spermatozoa also indicated for the first time a clear centrosomal localization of TTLL5, with no overlap with the polyglutamylated α - and β -tubulin of the flagellum.

DISCUSSION

Both primary (or immotile) and motile cilia play crucial roles in normal function of most tissues of the human body. These tiny hair-like organelles participate in a wide range of cellular functions during development, tissue morphogenesis and homeostasis. It is therefore not surprising that mutations in ciliary genes are often associated with a broad range of conditions, classified as ciliopathies, either involving single organs or causing syndromic phenotypes (8). Some examples of diseases affecting primary cilia are polycystic kidney disease, Usher syndrome, retinitis pigmentosa, Bardet-Biedl and Joubert syndromes (19-22). On the other hand, motile cilia defects have been shown to be causative for Kartagener syndrome and allied diseases, collectively grouped under the disease spectrum of primary ciliary dyskinesias.

Cilia and flagella, highly conserved in their core structure, are ancestral organelles composed of more than 650 proteins (10, 23). The building units of both cilia and flagella microtubules, α - and β -tubulin, are subject to post-translational modifications, accomplished by enzymes catalyzing different reactions such as the generation of $\Delta 2$ -tubulin, acetylation (24), tyrosination (25), polyglutamylation (26) and polyglycylation (27, 28). Among members of the TLL superfamily there are glutamylases and glycylicases (29-31). TLL5 initiates the formation of side chains within the C-terminal tail of α - and β -tubulin, with a preference for α -tubulin (32), and current models indicate that the role of polyglutamylation is to provide the necessary conditions for proper MT-MAPs (microtubule and microtubule-associated proteins) interactions. Studies have shown that polyglutamylation exerts differential regulation by selectively recruiting different MAPs: MAP1B, MAP2, tau, and neuronal kinesins have higher

affinity for tubulins with 1-3 glutamyl units, whereas MAP1A has higher affinity for longer side chains (25, 26, 28). Moreover, it has been shown that masking polyglutamylated sites with a specific anti-polyglutamylated tubulin antibody (GT335) affects the amplitude of flagellar beating in sea urchin sperm axonemes, suggesting a key role of polyglutamylated sites for interaction with ciliary dyneins (33). Centriole stability was also shown to be influenced by the degree of polyglutamylation, and GT335 antibody-loaded HeLa cells showed a complete transient disappearance of the centriole pair (13). Finally, members of the TLL family, *Tll3* and *Tll6*, play a role in cilia structure and motility in zebrafish (34). All TLL proteins have a preference for either α - or β -tubulin and participate to either initiation or elongation of the polyglutamyl side chain. TLL5, together with TLL4 and TLL7, initiates polyglutamylation, while other members function in the elongation of the polyglutamyl side chain or in the initiation or the elongation of polyglycylation.

Specific patterns of modifications on microtubules might be responsible of various functions. In the case of polyglutamylation, the side chains are built within the carboxy-terminal tail of tubulin, where the binding sites of motor and MT-associated proteins (MAPs) are also found. Thus, it is plausible that the interaction of MTs with such proteins might depend on specific patterns of modifications (35). Additional studies highlighted the importance of polyglutamylation for the proper beating of airway cilia (36), as well as for providing a molecular traffic sign required by motor proteins in order to maintain continuous synaptic transmission (37). Major evidence of the implication of polyglutamylation in photoreceptor ciliary function was recently reported (7), showing that *Tll5*^{-/-} mice developed a similar retinal phenotype to *Rpgr*^{-/-} mice, a known mouse model for retinitis

pigmentosa. In addition, *Ttll5*^{-/-} mice display strongly reduced glutamylation of RPGR^{ORF15}, a retina-specific variant of RPGR (38). Altogether, current evidence strongly supports the notion that the presence and length of polyglutamyl side chains, not only on tubulin but also on other substrates, is crucial for proper functioning of both motile and immotile cilia.

In our work we show that mutations in a gene involved in the polyglutamylation of α -tubulin is associated with defects in retina and spermatozoa. Clinically, these molecular phenotypes translate into cone-first CRD and reduced sperm motility, likely due to the functional impairment of the primary cilium and the flagellum, respectively. Our assumption is supported by immunofluorescence data, demonstrating that TLL5 localizes at the basal body of the cilia in photoreceptors, as well as at the base of the spermatozoal axoneme and in ciliated skin fibroblasts. Moreover, we reveal that the highest levels of expression of the major *TLL5* protein-coding isoform is in retina and testis. It is also very interesting to note that, in terms of fertility and *TLL5* pathogenic variants, there is an apparent genotype/phenotype correlation, which seems to be irrelevant for retinal degeneration. In other words, the phenotype elicited by *TLL5* pathogenic changes appears to depend on mutation classes. Missense variants are seemingly associated with a non-syndromic phenotype that is limited to the retina, whereas inactivating mutations appear to disrupt functions of both photoreceptors and spermatozoa, thus defining a novel allele-specific syndrome. Yet, three male patients with truncating *TLL5* mutations were previously reported having offspring (5), raising the possibility of variable expressivity or reduced penetrance of this class of mutations. In support of the latter hypothesis, *Ttll5* knockout mice display extremely reduced but not completely abolished

fertility (6). Alternatively, this genotype/phenotype correlation in our cohort could also be coincidental. The association of *TLL5* mutations with severe myopia is another intriguing hypothesis that warrants additional investigation in a larger cohort of patients, especially given the complex pattern of inheritance of nearsightedness in humans.

In conclusion, we show that mutations in *TLL5* are associated with a newly-defined syndrome affecting vision and the male reproductive system. Despite the fact that cilia and flagella have different morphologies and functions, they may share similar physiological mechanisms, and the enzymatic reaction of polyglutamylation performed by TLL5 may be one of these common elements.

MATERIALS AND METHODS

Patients and controls

Patient P1 was recruited from the Jules Gonin Ophthalmic Hospital (Lausanne, Switzerland); and patient P2 from the Department of Ophthalmology of Lund University Hospital (Lund, Sweden). Patients P3, P4 and P5 were recruited from the Radboud University Medical Center (Nijmegen, The Netherlands) and the Erasmus University Medical Center (Rotterdam, The Netherlands). Patients P6-8 were sampled by author MMK, an ophthalmologist based at St James's University Hospital (Leeds, England), while on a field trip in Pakistan. DNA of all subjects was extracted from peripheral blood leukocytes. A control sperm sample was provided by a healthy donor. Our research has been conducted in accordance with the tenets of the Declaration of Helsinki and was approved by the Institutional Review Boards of our respective Organizations.

Clinical evaluation

For patients P1-5, ophthalmologic examination included assessment of BCVA, slit-lamp examination, funduscopy, fundus photography, and optical coherence tomography. Full-field ERGs were also recorded, as prescribed by the International Society for Clinical Electrophysiology of Vision (ISCEV).

For patients P6-8, ophthalmologic assessment was limited to slit-lamp examination and fundus inspection using direct and indirect ophthalmoscopy through dilated pupils. Owing to the non-hospital setting, electrodiagnostic and other testing was not available. Visual acuity was recorded together with a history of nyctalopia or photoaversion.

Semen analysis was carried out for patients P1 and P2 by standard procedures of andrology laboratories, and according to WHO guidelines (39). For P1 patient, two Leja chambers (Leja) filled with 6 μ l of semen were entirely scanned under phase contrast microscopy to confirm the absence of spermatozoa. Additional clinical features were assessed only for patient P1, due to substantial problems in getting back to the other probands. These tests included a thorough otorhinolaryngology examination assessing structure and function of the nasopharyngeal mucosa, the ear canal and the hearing (by pure-tone audiometry), as well as a full renal examination, including a complete checkup of renal function, urine and blood analysis, assessment of blood pressure, and ultrasonography. Analyses involving other tissues and organs known to be involved in other ciliopathies were not performed due to a negative clinical history: normal body mass index, no respiratory complains, no metabolic disturbance and no skeletal abnormalities.

Whole Genome and Whole Exome Sequencing

WGS in the Swiss index patient P1 was performed using 4 μ g of DNA. Sequencing was performed by Complete Genomics Inc. (Mountain View, CA, USA), as described previously (40). Genetic variants were identified using v2.0 of the Complete Genomics pipeline (41). WES was performed for proband P6 using 3 μ g of DNA. Protein-coding regions were captured using the SureSelect All Exon v4 kit (Agilent, Santa Clara, CA, USA) and paired-end sequencing was performed using the Illumina HiSeq 2500 platform. Single nucleotide variants and small insertions or deletions were detected using the Genome Analysis Tool Kit (GATK v2.4.7) software package, using the Best Practice Guidelines identified by the developers

(42). The pathogenicity of genetic variants detected through WGS and WES were assessed after functional annotation through ANNOVAR (43).

Homozygosity mapping

Genomic regions with high homozygosity were determined using the free web based tool HomozygosityMapper (44).

Mutation screening

Primer pairs for *TLL5* exons and flanking intron boundaries were designed using the CLCbio Genomics Workbench (Qiagen, Table S2). PCR amplification was performed in a 20 μ l total volume containing 10 ng genomic DNA, 1x GoTaq buffer, 0.1 mM dNTPs, 10 μ M of each primer, and 5 U/ μ l of GoTag polymerase (Promega). PCR products were purified (ExoSAP-IT, USB) and a sequencing reaction was performed in a total volume of 5 μ l using 1 μ l primer 3.3 μ M, 0.5 μ l BigDye Terminator v1.1, and 1 μ l of the provided Buffer (Applied Biosystems).

Antibodies

Commercial goat polyclonal anti-TLL5 antibody (Santa Cruz Biotechnology Inc), raised against a peptide mapping near the C-terminus of TLL5 human origin, was used at a 1:100 dilution. Mouse monoclonal anti-centrin clone 20H5 antibody was purchased from Millipore and used at a dilution of 1:1000. Anti-polyglutamylated tubulin GT335 and monoclonal anti-acetylated tubulin antibodies were provided by Dr C. Janke (Institut Curie, Orsay, France) and purchased from Sigma-Aldrich, respectively. Secondary donkey anti-goat antibodies conjugated with Alexa Fluor 488 were purchased from Invitrogen and

secondary goat anti-mouse antibodies (Life Technologies) were conjugated with Alexa Fluor 594 (1:1000).

Fibroblast immortalization and culture

Primary skin fibroblasts were immortalized with exogenous hTERT by the use of pLOX-TERT-iresTK (45) and grown in DMEM(1x) + 1g/L D-glucose L-Glutamine Pyruvate (Gibco), supplemented with 10% FBS, 1% penicillin-streptomycin, and 1% fungizone, adapted from previously published protocols (46).

Immunofluorescence

Immunofluorescence was performed for TLL5 localization in human control spermatozoa and rat retinal sections. The sperm staining procedure used was adapted from a previously published protocol (47). After washing five times with PBS 1X in a 15 ml Falcon tube and centrifugation steps of 5' at 800g, all at room temperature (RT), the semen pellet was resuspended and fixed with 4% (v/w) PFA in PBS, and incubated for 30 minutes on ice. The sample was then washed three times with PBS and stored at 4°C for future use. The immunostaining procedure used 20 µl aliquots of fixed sperm cells, transferred to a 1.5 µl Eppendorf tubes. Blocking was done for 30 minutes at RT in 100 µl PBS containing 3% (w/v) BSA (PBSA). Primary antibody incubation was performed with specified dilutions in 100 µl PBSA, overnight at 4°C. Samples were washed three times with PBS containing 0.1% (v/v) TX100 (PBST). Secondary antibody incubation of 30 minutes was carried out at RT in 100 µl PBSAT [PBST containing 3% (w/v) BSA and 0.1% (v/v) TX100]. After three washes with PBST and two washes with PBS the final pellet was resuspended in PBS and 5 µl were placed on a slide. 5 µl DAPI

vectashield were added to the sample, which was then coverslipped and fixed with nail polish.

Unfixed Sprague-Dawley rat eyes and C57BL/6J mouse eyes were isolated and soaked for 3 hours in PBS containing 30% sucrose. Eyes were embedded in Yazulla medium (30% egg albumen and 3% gelatin in water) and cryosectioned (12 μ m) onto Superfrost Plus slides (Thermo Scientific). Sections were washed three times with PBS and a stepwise procedure was followed similarly to that described for sperm immunostaining, the only difference being that this was carried out on slide and with lower volumes.

Quantitative Real Time PCR

Primer pairs used for q-PCR are listed in Table S3. The q-PCR product was visualized on 1% agarose gel to verify primer's specificity. A standard curve using a control cDNA template prepared from human normal tissues total RNA (BioChain) was used to test the efficiency of each primer pair. *HPRT1* was used as a normalization control, as described (48). Amplification was performed using the SYBR Green PCR Master Mix (Applied Biosystems).

ACKNOWLEDGEMENTS

This work was supported by grants from the Swiss National Science Foundation to CR [grant numbers 138346, 156260], the Foundation Fighting Blindness USA to FPMC [grant number C-GE-0811-0545-RAD01], and RP Fighting Blindness and Fight For Sight [RP Genome Project GR586]. MEE was funded by an Egyptian Government Scholarship. Family F6 was analyzed by the UK Inherited Retinal Disease Consortium. We would like to thank the patients and their families who participated in this study.

CONFLICT OF INTEREST STATEMENT

The authors declare no conflict of interest.

REFERENCES

- 1 Hamel, C.P. (2007) Cone rod dystrophies. *Orphanet J. Rare Dis.*, **2**, 7.
- 2 Berson, E.L., Gouras, P. and Gunkel, R.D. (1968) Progressive cone-rod degeneration. *Arch. Ophthalmol.*, **80**, 68-76.
- 3 Berson, E.L., Gouras, P. and Gunkel, R.D. (1968) Progressive cone degeneration, dominantly inherited. *Arch. Ophthalmol.*, **80**, 77-83.
- 4 Roosing, S., Thiadens, A.A., Hoyng, C.B., Klaver, C.C., den Hollander, A.I. and Cremers, F.P. (2014) Causes and consequences of inherited cone disorders. *Prog. Retin. Eye Res.*, **42**, 1-26.
- 5 Sergouniotis, P.I., Chakarova, C., Murphy, C., Becker, M., Lenassi, E., Arno, G., Lek, M., MacArthur, D.G., Consortium, U.C.-E., Bhattacharya, S.S. *et al.* (2014) Biallelic variants in TLL5, encoding a tubulin glutamylase, cause retinal dystrophy. *Am. J. Hum. Genet.*, **94**, 760-769.
- 6 Lee, G.S., He, Y., Dougherty, E.J., Jimenez-Movilla, M., Avella, M., Grullon, S., Sharlin, D.S., Guo, C., Blackford, J.A., Jr., Awasthi, S. *et al.* (2013) Disruption of Tll5/stamp gene (tubulin tyrosine ligase-like protein 5/SRC-1 and TIF2-associated modulatory protein gene) in male mice causes sperm malformation and infertility. *J. Biol. Chem.*, **288**, 15167-15180.
- 7 Sun, X., Park, J.H., Gumerson, J., Wu, Z., Swaroop, A., Qian, H., Roll-Mecak, A. and Li, T. (2016) Loss of RPGR glutamylation underlies the pathogenic mechanism of retinal dystrophy caused by TLL5 mutations. *Proc. Natl. Acad. Sci. U. S. A.*, **113**, E2925-2934.
- 8 Hildebrandt, F., Benzing, T. and Katsanis, N. (2011) Ciliopathies. *N. Engl. J. Med.*, **364**, 1533-1543.

- 9 Waters, A.M. and Beales, P.L. (2011) Ciliopathies: an expanding disease spectrum. *Pediatr. Nephrol.*, **26**, 1039-1056.
- 10 Fliegau, M., Benzing, T. and Omran, H. (2007) When cilia go bad: cilia defects and ciliopathies. *Nat. Rev. Mol. Cell Biol.*, **8**, 880-893.
- 11 Hildebrandt, F., Attanasio, M. and Otto, E. (2009) Nephronophthisis: disease mechanisms of a ciliopathy. *J. Am. Soc. Nephrol.*, **20**, 23-35.
- 12 Schorderet, D.F., Bernasconi, M., Tiab, L., Favez, T. and Escher, P. (2014) IROme, a new high-throughput molecular tool for the diagnosis of inherited retinal dystrophies-a price comparison with Sanger sequencing. *Adv. Exp. Med. Biol.*, **801**, 171-176.
- 13 Bobinnec, Y., Khodjakov, A., Mir, L.M., Rieder, C.L., Edde, B. and Bornens, M. (1998) Centriole disassembly in vivo and its effect on centrosome structure and function in vertebrate cells. *J. Cell Biol.*, **143**, 1575-1589.
- 14 Firmann, M., Mayor, V., Vidal, P.M., Bochud, M., Pecoud, A., Hayoz, D., Paccaud, F., Preisig, M., Song, K.S., Yuan, X. *et al.* (2008) The CoLaus study: a population-based study to investigate the epidemiology and genetic determinants of cardiovascular risk factors and metabolic syndrome. *BMC Cardiovasc. Disord.*, **8**, 6.
- 15 Lek, M., Karczewski, K., Minikel, E., Samocha, K., Banks, E., Fennell, T., O'Donnell-Luria, A., Ware, J., Hill, A., Cummings, B. *et al.* (2015) Analysis of protein-coding genetic variation in 60,706 humans. *bioRxiv*.
- 16 Sherry, S.T., Ward, M.H., Kholodov, M., Baker, J., Phan, L., Smigielski, E.M. and Sirotkin, K. (2001) dbSNP: the NCBI database of genetic variation. *Nucleic Acids Res.*, **29**, 308-311.

- 17 KDIGO (2013) Clinical Practice Guideline for the Evaluation and Management of Chronic Kidney Disease. *Kidney Int Suppl* (2013), **3**, 150.
- 18 Hentze, M.W. and Kulozik, A.E. (1999) A perfect message: RNA surveillance and nonsense-mediated decay. *Cell*, **96**, 307-310.
- 19 Badano, J.L., Mitsuma, N., Beales, P.L. and Katsanis, N. (2006) The ciliopathies: an emerging class of human genetic disorders. *Annu Rev Genomics Hum Genet*, **7**, 125-148.
- 20 Zaghoul, N.A. and Katsanis, N. (2009) Mechanistic insights into Bardet-Biedl syndrome, a model ciliopathy. *J. Clin. Invest.*, **119**, 428-437.
- 21 Forsythe, E. and Beales, P.L. (2013) Bardet-Biedl syndrome. *Eur. J. Hum. Genet.*, **21**, 8-13.
- 22 Falk, N., Losl, M., Schroder, N. and Giessl, A. (2015) Specialized Cilia in Mammalian Sensory Systems. *Cells*, **4**, 500-519.
- 23 Carvalho-Santos, Z., Azimzadeh, J., Pereira-Leal, J.B. and Bettencourt-Dias, M. (2011) Evolution: Tracing the origins of centrioles, cilia, and flagella. *J. Cell Biol.*, **194**, 165-175.
- 24 Piperno, G. and Fuller, M.T. (1985) Monoclonal antibodies specific for an acetylated form of alpha-tubulin recognize the antigen in cilia and flagella from a variety of organisms. *J. Cell Biol.*, **101**, 2085-2094.
- 25 Gundersen, G.G. and Bulinski, J.C. (1986) Distribution of tyrosinated and nontyrosinated alpha-tubulin during mitosis. *J. Cell Biol.*, **102**, 1118-1126.
- 26 Edde, B., Rossier, J., Le Caer, J.P., Desbruyeres, E., Gros, F. and Denoulet, P. (1990) Posttranslational glutamylation of alpha-tubulin. *Science*, **247**, 83-85.
- 27 Westermann, S. and Weber, K. (2003) Post-translational modifications regulate microtubule function. *Nat. Rev. Mol. Cell Biol.*, **4**, 938-947.

- 28 Janke, C. and Kneussel, M. (2010) Tubulin post-translational modifications: encoding functions on the neuronal microtubule cytoskeleton. *Trends Neurosci.*, **33**, 362-372.
- 29 Boucher, D., Larcher, J.C., Gros, F. and Denoulet, P. (1994) Polyglutamylation of tubulin as a progressive regulator of in vitro interactions between the microtubule-associated protein Tau and tubulin. *Biochemistry*, **33**, 12471-12477.
- 30 Larcher, J.C., Boucher, D., Lazereg, S., Gros, F. and Denoulet, P. (1996) Interaction of kinesin motor domains with alpha- and beta-tubulin subunits at a tau-independent binding site. Regulation by polyglutamylation. *J. Biol. Chem.*, **271**, 22117-22124.
- 31 Bonnet, C., Boucher, D., Lazereg, S., Pedrotti, B., Islam, K., Denoulet, P. and Larcher, J.C. (2001) Differential binding regulation of microtubule-associated proteins MAP1A, MAP1B, and MAP2 by tubulin polyglutamylation. *J. Biol. Chem.*, **276**, 12839-12848.
- 32 Janke, C., Rogowski, K., Wloga, D., Regnard, C., Kajava, A.V., Strub, J.M., Temurak, N., van Dijk, J., Boucher, D., van Dorselaer, A. *et al.* (2005) Tubulin polyglutamylase enzymes are members of the TTL domain protein family. *Science*, **308**, 1758-1762.
- 33 Gagnon, C., White, D., Cosson, J., Huitorel, P., Edde, B., Desbruyeres, E., Paturle-Lafanechere, L., Multigner, L., Job, D. and Cibert, C. (1996) The polyglutamylated lateral chain of alpha-tubulin plays a key role in flagellar motility. *J. Cell Sci.*, **109 (Pt 6)**, 1545-1553.

- 34 Pathak, N., Austin, C.A. and Drummond, I.A. (2011) Tubulin tyrosine ligase-like genes *tll3* and *tll6* maintain zebrafish cilia structure and motility. *J. Biol. Chem.*, **286**, 11685-11695.
- 35 Janke, C., Rogowski, K. and van Dijk, J. (2008) Polyglutamylation: a fine-regulator of protein function? 'Protein Modifications: beyond the usual suspects' review series. *EMBO Rep*, **9**, 636-641.
- 36 Ikegami, K., Sato, S., Nakamura, K., Ostrowski, L.E. and Setou, M. (2010) Tubulin polyglutamylation is essential for airway ciliary function through the regulation of beating asymmetry. *Proc. Natl. Acad. Sci. U. S. A.*, **107**, 10490-10495.
- 37 Ikegami, K., Heier, R.L., Taruishi, M., Takagi, H., Mukai, M., Shimma, S., Taira, S., Hatanaka, K., Morone, N., Yao, I. *et al.* (2007) Loss of alpha-tubulin polyglutamylation in ROSA22 mice is associated with abnormal targeting of KIF1A and modulated synaptic function. *Proc. Natl. Acad. Sci. U. S. A.*, **104**, 3213-3218.
- 38 Vervoort, R., Lennon, A., Bird, A.C., Tulloch, B., Axton, R., Miano, M.G., Meindl, A., Meitinger, T., Ciccodicola, A. and Wright, A.F. (2000) Mutational hot spot within a new RPGR exon in X-linked retinitis pigmentosa. *Nat. Genet.*, **25**, 462-466.
- 39 WHO (2010) *WHO laboratory manual for the examination and processing of human semen*.
- 40 Drmanac, R., Sparks, A.B., Callow, M.J., Halpern, A.L., Burns, N.L., Kermani, B.G., Carnevali, P., Nazarenko, I., Nilsen, G.B., Yeung, G. *et al.* (2010) Human genome sequencing using unchained base reads on self-assembling DNA nanoarrays. *Science*, **327**, 78-81.
- 41 Carnevali, P., Baccash, J., Halpern, A.L., Nazarenko, I., Nilsen, G.B., Pant, K.P., Ebert, J.C., Brownley, A., Morenzoni, M., Karpinchyk, V. *et al.* (2012) Computational

techniques for human genome resequencing using mated gapped reads. *J. Comput. Biol.*, **19**, 279-292.

42 DePristo, M.A., Banks, E., Poplin, R., Garimella, K.V., Maguire, J.R., Hartl, C., Philippakis, A.A., del Angel, G., Rivas, M.A., Hanna, M. *et al.* (2011) A framework for variation discovery and genotyping using next-generation DNA sequencing data. *Nat. Genet.*, **43**, 491-498.

43 Wang, K., Li, M. and Hakonarson, H. (2010) ANNOVAR: functional annotation of genetic variants from high-throughput sequencing data. *Nucleic Acids Res.*, **38**, e164.

44 Seelow, D., Schuelke, M., Hildebrandt, F. and Nurnberg, P. (2009) HomozygosityMapper--an interactive approach to homozygosity mapping. *Nucleic Acids Res.*, **37**, W593-599.

45 Salmon, P., Oberholzer, J., Occhiodoro, T., Morel, P., Lou, J. and Trono, D. (2000) Reversible immortalization of human primary cells by lentivector-mediated transfer of specific genes. *Mol. Ther.*, **2**, 404-414.

46 van Karnebeek, C.D., Bonafe, L., Wen, X.Y., Tarailo-Graovac, M., Balzano, S., Royer-Bertrand, B., Ashikov, A., Garavelli, L., Mammi, I., Turolla, L. *et al.* (2016) NANS-mediated synthesis of sialic acid is required for brain and skeletal development. *Nat. Genet.*, **48**, 777-784.

47 Nishimura, H., Gupta, S., Myles, D.G. and Primakoff, P. (2011) Characterization of mouse sperm TMEM190, a small transmembrane protein with the trefoil domain: evidence for co-localization with IZUMO1 and complex formation with other sperm proteins. *Reproduction*, **141**, 437-451.

48 Hoggart, C.J., Venturini, G., Mangino, M., Gomez, F., Ascari, G., Zhao, J.H., Teumer, A., Winkler, T.W., Tsernikova, N., Luan, J. *et al.* (2014) Novel approach

identifies SNPs in SLC2A10 and KCNK9 with evidence for parent-of-origin effect on body mass index. *PLoS Genet.*, **10**, e1004508.

LEGENDS TO FIGURES

Figure 1: Pedigrees from families with pathogenic *TTL5* variants. The probands are: subject P1 [II:3, family F1; c.1782del;p.(Asp594Glufs*29)], subject P2 [II:4, family F2; c.349C>T;p.(Gln117*)], subject P3 [II:3, family F3; c.2132_2133insGATA;p.(Met712IleAspfs*15)], subject P4 [II:4, family F4; c.1627G>A;p.(Glu543Lys)], subject P5 [II:4, family F5; c.2266A>T;p.(Ile756Phe)], and subject P6 [IV:14, family F6; c.1627G>A;p.(Glu543Lys)].

Figure 2: Fundi of index patient P1. Autofluorescence imaging of the right (A) and left (B) eye at age 66 years, showing a distinctive pattern of abnormalities, including a hyperfluorescent ring and hyperfluorescent area at the fovea surrounded by patchy hypofluorescence in both eyes. Hypofluorescence around the optic nerve was also present. The same images, obtained 6 years later (C, D), showed an increase of hypofluorescent areas within the ring and a mild enlargement of the hyperfluorescent ring in both eyes. Composite pictures of the fundi at age 72, showing atrophic areas around the fovea and around the optic nerve (E, F). Peripheral retina was within normal limits.

Figure 3: Mutation diagram of the *TTL5* protein (A), and corresponding cDNA. Exons are numbered and drawn to scale (B) with respect to the protein sequence. The TTL domain responsible for polyglutamylation activity is indicated. Chromatograms of the mutations identified (C), compared to their relevant wild type sequences (D).

Figure 4: Relative expression of *TLL5* isoforms and their expression. *TLL5* has six known alternative transcripts (001, 002, 003, 016, 017, and 018), resulting from the splicing of the exons indicated here in dark grey (A). Their expression within seven different human tissues, measured by quantitative real time PCR, is indicated by both numerical values and shades of grey (B). Although all isoforms seem to be widely expressed, isoform 001 is the most prominent one, among all tissues considered ('Total' column). Asterisks show the position of the mutations identified in this work.

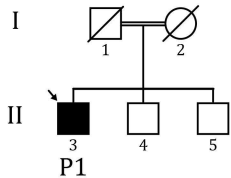
Figure 5: *TLL5* isoform 001 expression in fibroblasts of the index patient P1 vs. a control, by quantitative PCR. *TLL5* mRNA amounts were normalized with respect to the housekeeping gene *HPRT1*.

Figure 6: Immunofluorescence staining of ciliated control human skin fibroblasts (A-D). *TLL5* co-localizes with acetylated tubulin at the centrioles, as indicated by arrowheads (C, D). Immunofluorescence in rat retina sections (E, and magnified cilium in F) and in control human spermatozoon (G). *TLL5* decorates the basal body in photoreceptors and the centrioles in spermatozoa. Scale bars: A-E, 5 μm ; B, 1 μm ; C, 20 μm .

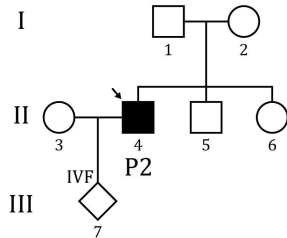
Table 1 : patients with TLL5 mutations and clinical features

Family	Patient	TLL5 protein change	Zygoty	Sex	Age at last examination	Visual acuity	Correction	Full field ERG at last examination		Macula	Periphery	Other features
								cone response	rod response			
F1	P1	c.1782del; p.Asp594Glufs*29	hom	M	75	0.05	-3.6	absent	reduced	atrophy	normal	azoospermia
F2	P2	c.349C>T; p.Gln117*	hom	M	46	0.05	-10.00	residual	residual	atrophy	minor changes	reduced motility of sperm; normal anterior eye segment
F3	P3	c.2132_2133insGATA; p.Met712IleAspfs*15	hom	F	58	0.16	-3	reduced	normal		normal	
F4	P4	c.1627G>A; p.Glu543Lys	hom	M	61	0.03	-5	absent	normal	atrophy	normal	
F5	P5	c.2266A>T; p.Ile756Phe	hom	M	38	0.33	-8	absent	normal	pigmentary changes	normal	
F6	P6	c.1627G>A; p.Glu543Lys	hom	M	53	NA	-8.00	NA	NA	atrophy	pigmentary changes	phthisical right eye
	P7	c.1627G>A; p.Glu543Lys	hom	M	38	NA	-5.00	NA	NA	NA	NA	posterior subcapsular cataract
	P8	c.1627G>A; p.Glu543Lys	hom	M	18	NA	-22.00	NA	NA	NA	NA	fairly normal retina

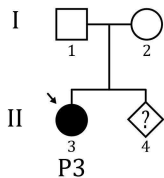
F1



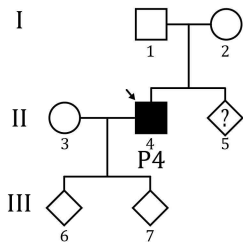
F2



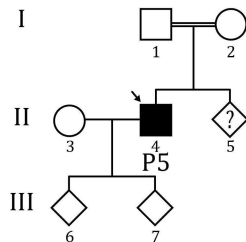
F3



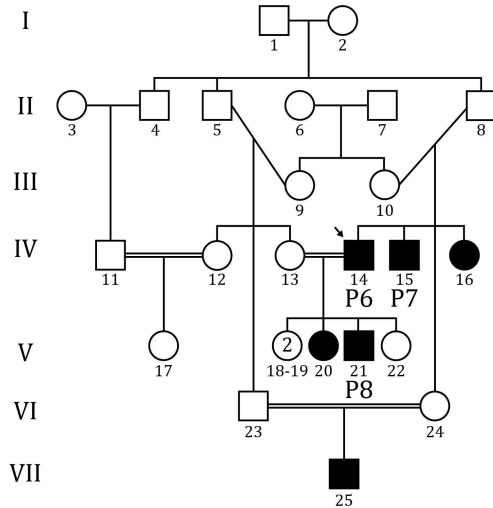
F4

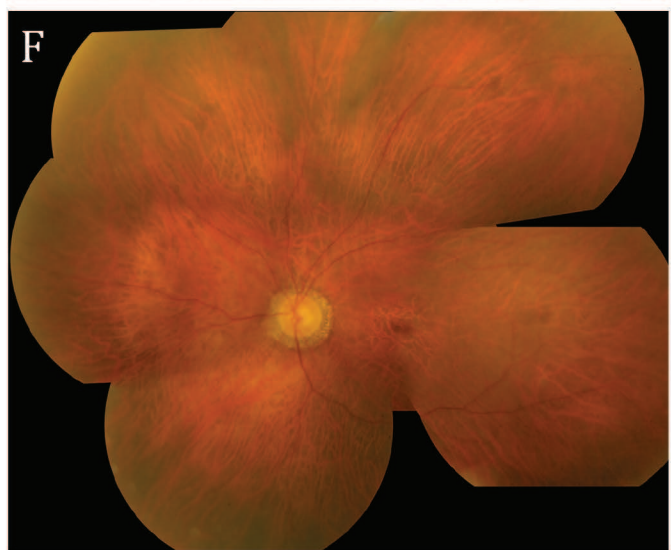
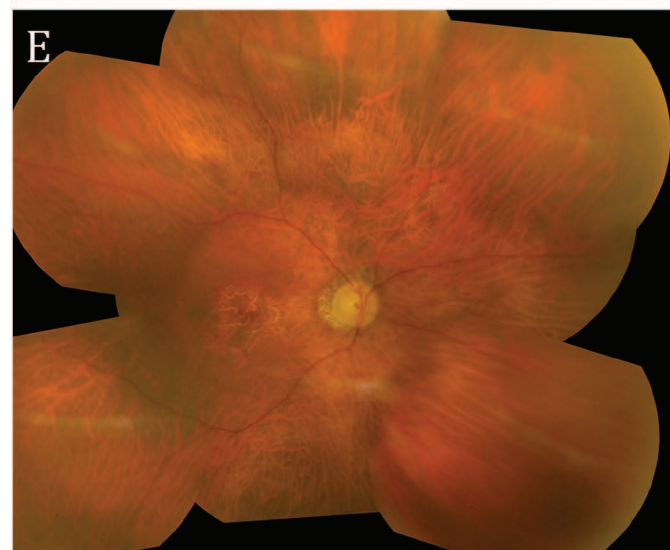
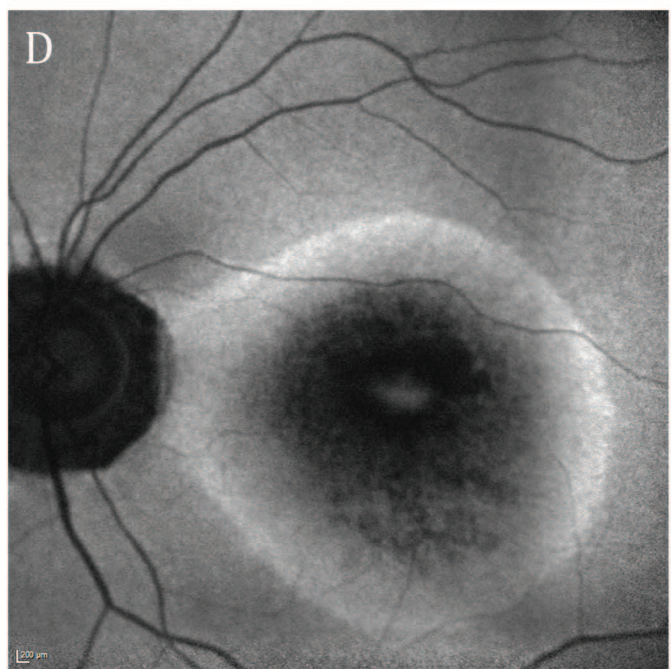
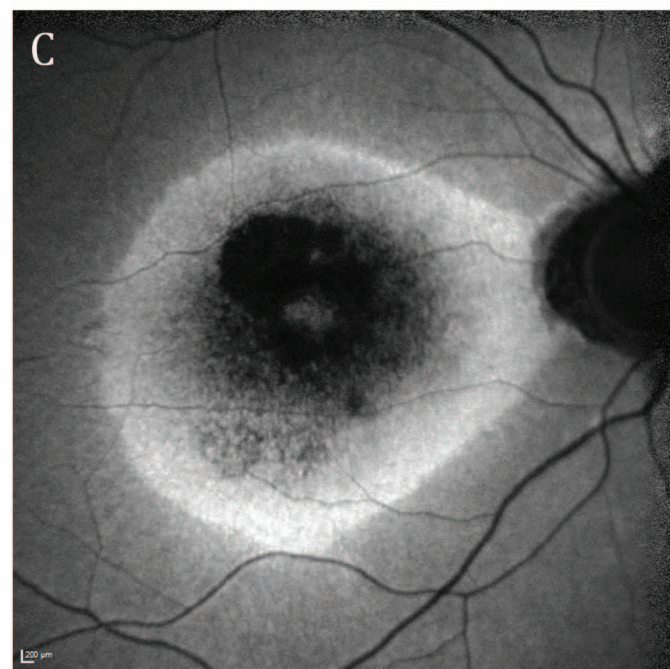
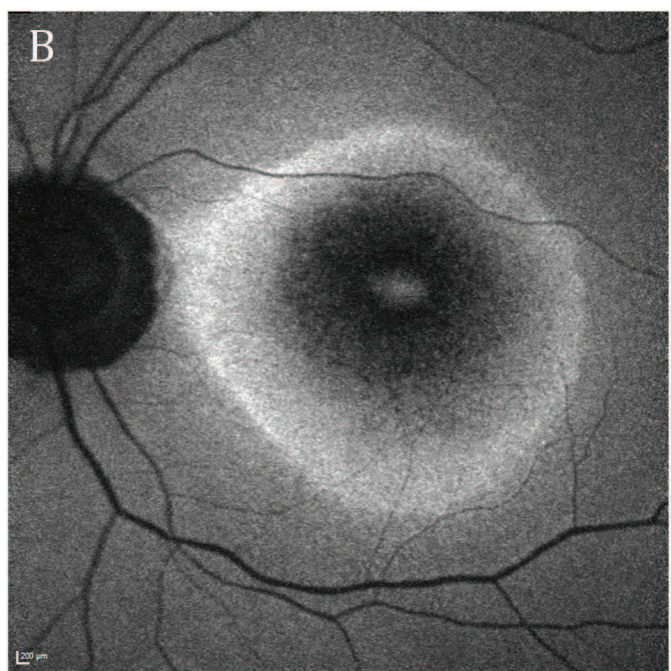
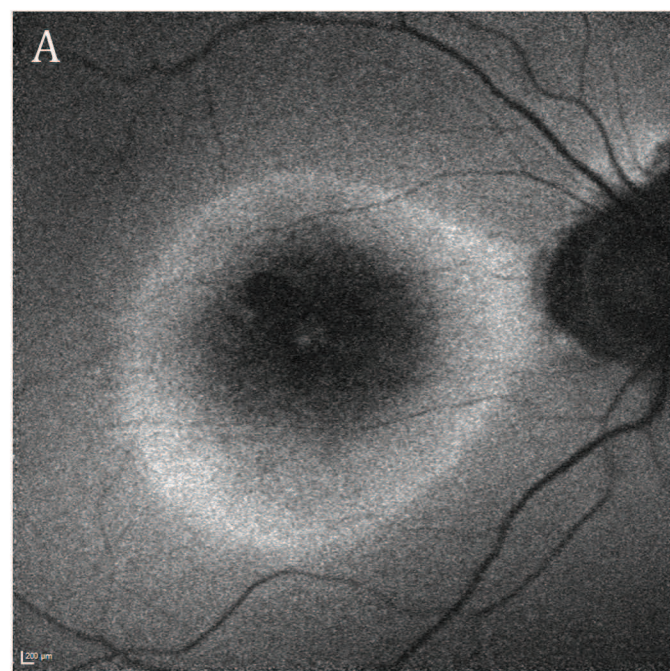


F5

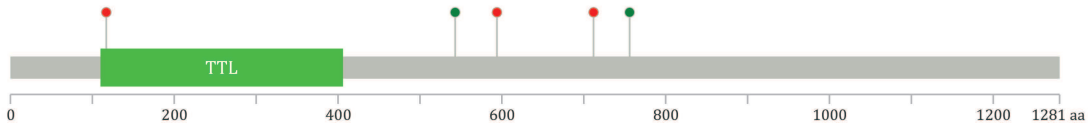


F6





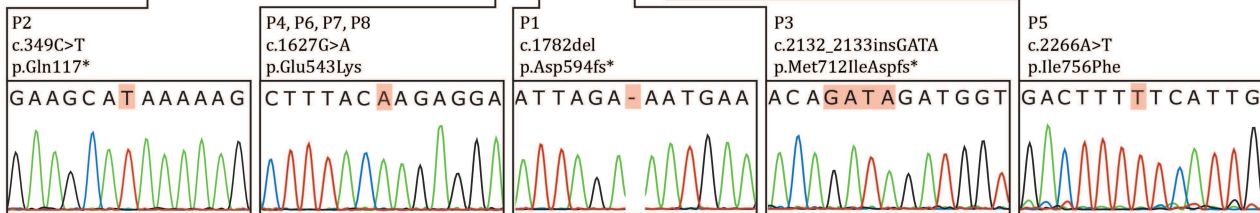
A



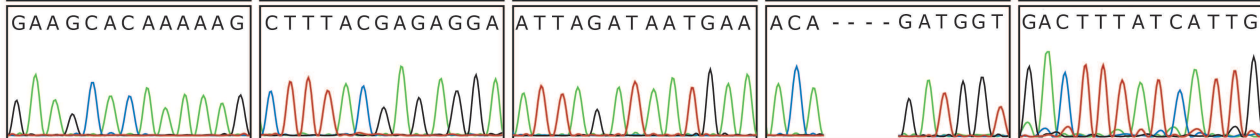
B

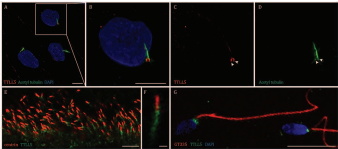


C

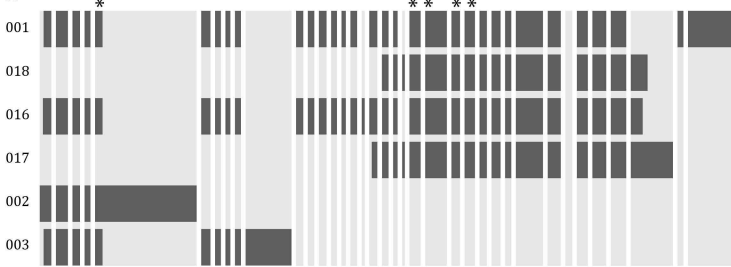


D





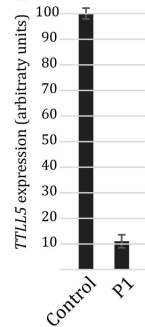
A



B



C



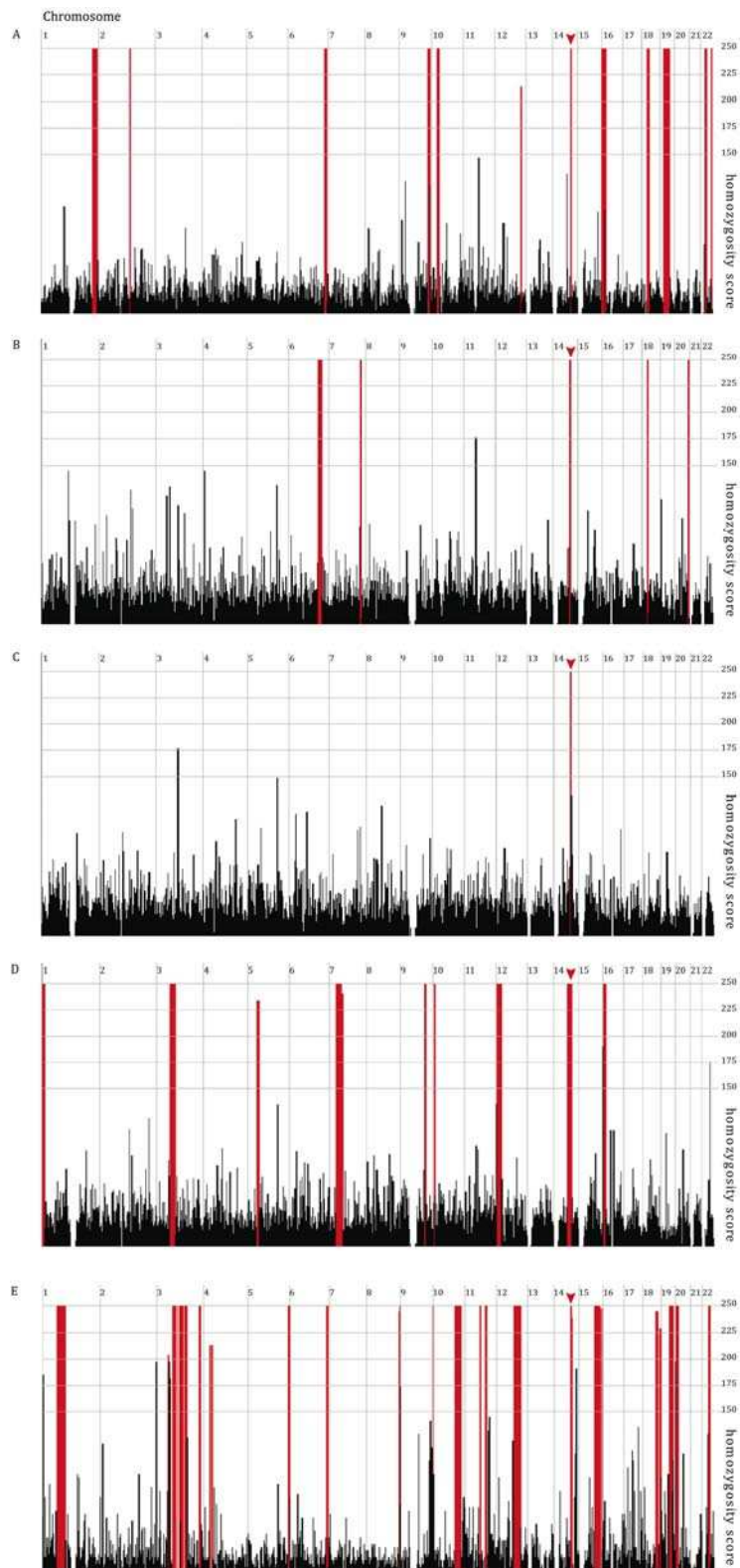


Figure S1: Autozygous regions of patients P1, P3, P4, P5, and P6 (panels A, B, C, D, and E, respectively). In all these patients, *TLL5* lies in a region of homozygosity (red arrowhead).

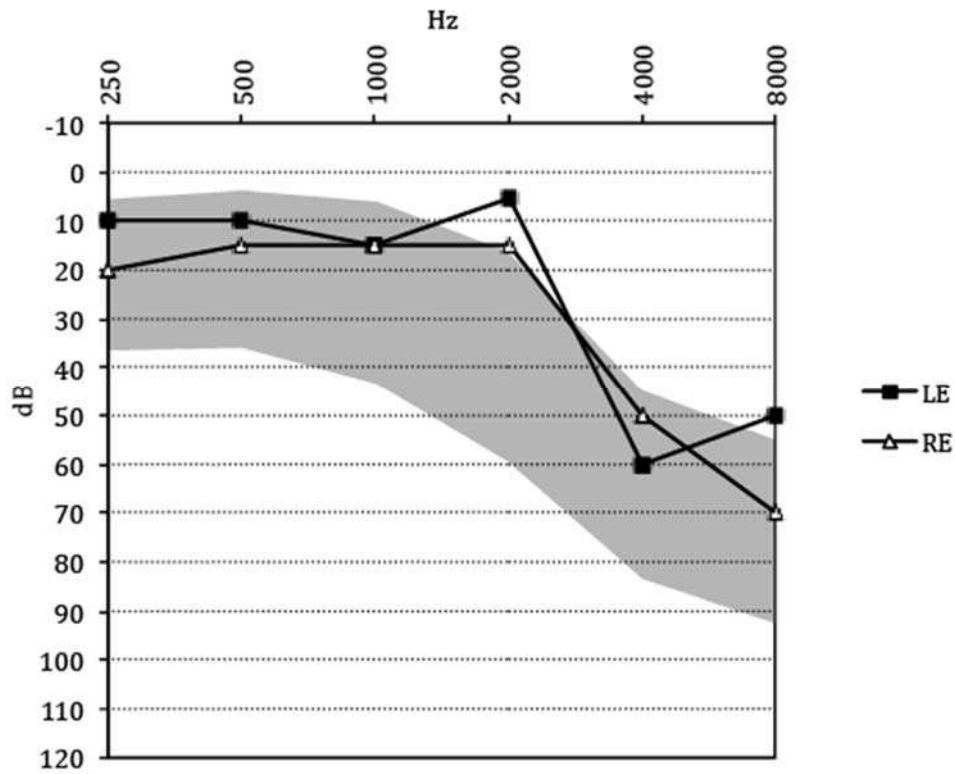


Figure S2: Pure-tone conduction audiograms for the index patient P1. Data is shown separately for the left and right ear (LE and RE, respectively). The grey area depicts the hearing ranges (average values ± 1 standard deviation) for normal male individuals at age 70-79, as reported by Cruickshanks *et al.* (1998).

Table S1: WGS data (index patient P1)

Filtering step	Variants
total called variants	4,043,185
homozygous	1,418,251
exonic	8,486
non synonymous	3,892
not in 69 WGS healthy controls	90
not in dbSNP132	19

Table S2: Primers used for the screening of *TLL5* exons and flanking sequences

Exon					Amplicon size [bp]	Annealing T [°C]
E1 (5'-UTR)						
E2	F	5'-	ATTGAGGCACATATTGAGG	-3'	470	55
	R	5'-	CCCAAGGAATGACACTAGA	-3'		
E3	F	5'-	CAGAAGGAAGGGGAAACTTG	-3'	391	55
	R	5'-	CAGAGGAAAAACATAAGCAG	-3'		
E4	F	5'-	CTCATGGTCCAAAATACGTTCA	-3'	292	55
	R	5'-	TAGGTGGCTGGGATTTTCAG	-3'		
E5	F	5'-	GGTGAGTACACTGTGGATGAAA	-3'	301	57
	R	5'-	AGGACACTAATTACCTTTGCTG	-3'		
E6	F	5'-	TCTAGGACTGTGAACTGTA ACT	-3'	327	55
	R	5'-	TTTGGAAGCCCTGATTGGT	-3'		
E7	F	5'-	GTTACTGCCAACACTTAG	-3'	288	55
	R	5'-	CAATACAAAGGGTGAAGGAG	-3'		
E8	F	5'-	AGA ACTTTGCTCCCTTATTG	-3'	284	57
	R	5'-	AACCTGCTGCCTTTCTGGA	-3'		
E9	F	5'-	TCCGAAGTCAAGGTGTGTG	-3'	454	56
	R	5'-	GAGACTACAGACAAATAAGCC	-3'		
E10	F	5'-	TTCATTGATCCTCAGTTC	-3'	290	59
	R	5'-	CACCTCTACAACCCACATC	-3'		
E11	F	5'-	CCTTCTCCCCACCCTCTTG	-3'	428	59
	R	5'-	CAGCAACTATCAAAGCAAC	-3'		
E12	F	5'-	TATAGCACCCATT CAGAAGTC	-3'	339	56
	R	5'-	GAATCACTAAGCCTCTCTACC	-3'		
E13	F	5'-	TCTCTGCTTCTACTTCCACTTG	-3'	320	56
	R	5'-	AAACAGTCTTCTAGTGCCAA	-3'		
E14	F	5'-	GGCTTTATGTGTTGCTCTTC	-3'	414	56
	R	5'-	CTCCTAATTCCTGTGCCTCA	-3'		
E15	F	5'-	TTATGGTGGTTCAGAGTTCAG	-3'	392	56
	R	5'-	CCAAATTCTCCTGCTCTAAGT	-3'		
E16	F	5'-	AAGTGGGCTATGAATTTGAG	-3'	845	56
	R	5'-	GGATAGGAAGCTAGTTAGGAG	-3'		
E17	F	5'-	TCTCCCTTCATGCTACTTTC	-3'	437	56
	R	5'-	E16 Reverse	-3'		
E18	F	5'-	CTGTCTTTTCCTTTGCCACT	-3'	354	56
	R	5'-	AGCATGCTTTCTACAGGACT	-3'		
E19	F	5'-	CTAGTGTTCTCTTTATCTGTC	-3'	420	56
	R	5'-	AGGTGTATGTGATCAGGAAG	-3'		
E20	F	5'-	GAAGGTATTGGGAGAGAGGAAC	-3'	608	59
	R	5'-	AAATGCCCAACCAATGAGAC	-3'		
E21	F	5'-	CCATCATAATAGAAGCATCCTC	-3'	452	56
	R	5'-	TGAACATAGCTCCAGGTCA	-3'		
E22	F	5'-	GTTCTGGGTCTTGTTTGTTG	-3'	299	56
	R	5'-	GCCAGAGAACAGAAGAAGAG	-3'		
E23	F	5'-	GGTGGCAAAAGTACATAAAG	-3'	395	56
	R	5'-	AGA ACTAAAGGGGTGTGCCA	-3'		
E24	F	5'-	AGGGAATTTTCAGCTTGTGC	-3'	412	56
	R	5'-	TACTGTCCCCCATTCTCCAC	-3'		
E25	F	5'-	TTAGGGCTGTGGGTGTCTTC	-3'	502	56
	R	5'-	CCCCTTCTTTTCACCCTTCT	-3'		

E26	F	5'-	GTTGTTTCTGGTAGGCAAA	-3'	654	56
	R	5'-	AAAGGCAAAGGGAAGAGATGA	-3'		
E27	F	5'-	GGCAGTTTGGTAATAGGAAG	-3'	497	56
	R	5'-	AAGAGGCATCAGTATATGGGA	-3'		
E28	F	5'-	TTCCTTCCTGAGTGCCTTTG	-3'	427	56
	R	5'-	CAGGTGGAGAAAGGGCATAT	-3'		
E29	F	5'-	ACTGTGCTTGGTTCCATATTG	-3'	338	56
	R	5'-	CCTACATTTCTCATTCACTG	-3'		
E30	F	5'-	CTGGCAACATTAGAGAAGT	-3'	502	56
	R	5'-	TTAGCCTTTATTTCCCAGCAG	-3'		
E31	F	5'-	AAGGAAGTGAGTGAATGAGCCA	-3'	348	56
	R	5'-	TGCCCATTTGCCAATGTTTT	-3'		
E32	F	5'-	CCACTTAGAGGTGAACTTCAT	-3'	394	56
	R	5'-	CCACTGCCAAGTTCCATCAAAA	-3'		

Table S3: Primers for q-PCR, specific for the six *TLL5* isoforms (Ensembl IDs)

Isoform					Amplicon size [bp]	Annealing T [°C]
001	F	5'-	CAACATCCCAGAAAGCTTCCAA	-3'	101	58
	R	5'-	TTTGTAGTGTGAGCAGGATCTGT	-3'		
002	F	5'-	CCACCTGAAGCCCTTCTTAC	-3'	144	58
	R	5'-	AGGACACTAATTACCTTTGCTG	-3'		
003	F	5'-	CCTCTATGTGCTCGTGACTTC	-3'	129	58
	R	5'-	AGCACCTGTACATAAATAGG	-3'		
016	F	5'-	GCCAATTTATCCCACCTTTGAG	-3'	85	58
	R	5'-	TTTGACGACTGAACTGTGCAG	-3'		
017	F	5'-	TCTGTGCTTGGTCTGTCAAT	-3'	200	58
	R	5'-	TAAGCTTCTTCTTGGGTTTCC	-3'		
017+018	F	5'-	TCGGCGAGGTGGATTTATTC	-3'	148	58
	R	5'-	TCCTGTCAATAAGCTTCTTC	-3'		